



WWJMRD 2021; 7(3): 1-9

www.wwjmr.com

International Journal

Peer Reviewed Journal

Refereed Journal

Indexed Journal

Impact Factor SJIF 2017:

5.182 2018: 5.51, (ISI) 2020-

2021: 1.361

E-ISSN: 2454-6615

**Manu Faujdar, Sushila**  
Department of Physics,  
Vivekananda Global  
University, Jaipur, India.

## Synthesis and study of optical properties of Zinc Copper Oxide doped PMMA composites

**Manu Faujdar, Sushila**

### Abstract

We have developed Pure Zinc Oxide (ZnO) and Pure Copper Oxide (CuO) and mixed Zinc-Copper oxide with five different ratios viz. 2-10gm, 4-10gm, 6-10gm, 8-10gm, 10-10gm in wt% by Sol-Gel technique then we have developed Pure PMMA and prepared Pure ZnO, CuO and mixed Zinc-Copper oxide doped PMMA films by weight percentage of 9%. Prepared material doped PMMA composite films of thickness (~100  $\mu\text{m}$ ) using the solution-cast technique. To spot the possible change that happen to the PMMA films as a result of doping, the optical properties were investigated for various wt.% ratios of Zinc, Copper, mixed Zinc-Copper oxide materials by recording the absorbance and transmittance spectra of those films using EI2375 double beam UV-Vis spectrophotometer within the wavelength range of 300–1100 nm. From the info obtained from the optical parameters viz. coefficient of absorption, extinction coefficient, finesse coefficient, refractive index, real and imaginary parts of dielectric constant and optical conductivity were calculated for the prepared films. The indirect optical band gap for the pure and therefore the doped-PMMA films were also calculated.

**Keywords:** Optical parameters mixed metal oxide, Zn-CuO –PMMA composites.

### Introduction

Nanotechnology is most likely going to have a significant effect on our economy and society inside the mid twenty-first century, science and innovation research in nanotechnology guarantees achievements in such regions as materials and assembling, nano gadgets, medication and medical services, energy, biotechnology, information technology, and national security. It's widely felt that nanotechnology are going to be subsequent technological revolution. [1-3] Polymer nano composites have unique properties like light weight, high flexibility, and skill to be fabricated at low temperature and low price. Polymers are of significant interest to society and are supplanting metals in different fields of life, which may be further modified consistent with modern application. They are more desirable than traditional materials in such areas as packaging, construction, and medical applications. Processing of polymeric materials basically depends on applied heat and pressure. [1] A material is basically a combination of at least two materials, every one of which holds its own distinctive properties. Normally the term composite is applied to materials that are made by mechanical holding of at least two unique materials together. The polymer has astounding optical properties but has poor scratch properties. It's acceptable dimensional stability because of rigid polymer chains. It's weather resistance and is steady to corrosive and soluble bases. It attacked by a few natural solvents, and has great effect strength higher, than that of glass or polystyrene. It's the least difficult straightforwardness and optical properties of commercially accessible thermoplastic. PMMA may be a colorless transparent plastic, i.e. transmits light almost perfectly (92%), which make them suitable to function a conduit for light. Dichloromethane, which is as a dissolvent for PMMA, is taken into account because the greatest soluble limit for PMMA; it's the best evaporation rates, less viscosity and therefore the least chemical hazard than other solvents [4- 6]. Oxide (CuO) nanoparticles are prominent due to their varied applications in superconductors, optical, electrical, catalytic, photo catalytic degradation, gas sensors, and in biosensors. CuO is an antimicrobial, anti-biotic and anti- fungal agent when

### Correspondence:

**Manu Faujdar, Sushila**  
Department of Physics,  
Vivekananda Global  
University, Jaipur, India.

incorporated in coatings, plastics, textiles, etc. It performs as a catalyst to eliminate industrial effluent within the environment. The elimination of those pigments and other organic materials ensures a secure and clean environment. The optical properties of anisotropic semiconductors are the topic of the many recent papers. The study of the optical constants of materials composite is interesting for several reasons. First, the utilization of materials in reflected coating requires accurate knowledge and optical fibers of their optical constants over wide ranges of wavelength. Second, the optical properties of all materials are associated with their electronic band structure, atomic structure and electrical properties. The optical properties of polymers are often suitably modified by the adding of dopants tally on their reactivity with the Amphitryon matrix [7, 8]. ZnO nanoparticles have attracted much attention thanks to the strong commercial desire for photo catalysis, photo electrochemistry, blue and UV light emitters and detectors supported their specific properties. The UV emission is attributed to the exciton radiative recombination while that of the visible emission still remains uncertain. Various mechanisms are proposed, in fact, most probable origin of the visible PL is caused by the intrinsic defects. The density of those defects has got to be higher on the surface of the sample, first of all due to the zinc and oxygen vacancies. Within the case of nanoparticles, the influence of surface is predicted to be more pronounced due to the increased surface-to-volume ratio.[9]

Earlier the authors have studied the optical properties of potassium chromate, [10] potassium permanganate ( $\text{KMnO}_4$ ), [11] Tin Chloride ( $\text{SnCl}_2$ ) [12] doped poly (methylmethacrylate) (PMMA) composite films and in all these literature author said optical parameters significantly changes with all dopant material. Enthralled from the results obtained we were motivated to investigate and hence reported here. in this paper we report the method of preparation of ZnO and CuO nanoparticle and Zn-CuO/PMMA nanocomposite film preparation as well as the investigation of comparative optical properties of pure ZnO/PMMA, CuO /PMMA and mixed Zn-CuO/PMMA.

## Experimental

**Chemical involved:** Zinc chloride ( $\text{ZnCl}_2$ ), copper chloride ( $\text{CuCl}_2$ ) and dichloromethane of analytical grade were purchased from Merck Specialties Pvt. Ltd, "Mumbai; PMMA granules were purchased from M/s Gadra Chemicals Bharuch"; distilled water and ethyl alcohol ( $\text{C}_2\text{H}_5\text{OH}$ ) were purchased from Himedia Laboratories, Mumbai. All these chemicals were used without purification or as received.

**Synthesis of Zinc oxide nano-particles by sol-gel technique:** Zinc Chloride ( $\text{ZnCl}_2$ ) and sodium hydroxide ( $\text{NaOH}$ ) were the two starting materials for preparation of zinc oxide particles. We took a 5gm of  $\text{NaOH}$  in distilled water and stirred it at 50 degree centigrade in a beaker on a magnetic stirrer. After that we took an 8.5 gm of Zinc chloride in distilled water in a beaker and keep stirred it on another magnetic stirrer.  $\text{ZnCl}_2$  solution added in  $\text{NaOH}$  solution drop wise continuously and allowed to stirring. The doping of the  $\text{ZnCl}_2$  solution in an aqueous alkaline solution results in instant precipitation of ZnO, and color changes from transparent to white. Precipitated was washed

for five times with distilled water for the complete removal of residues from the suspension. Then, the final precipitates were achieved after drying.

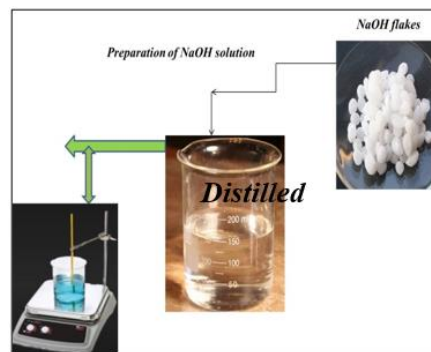


Fig. 1: Preparation of NaOH solution.

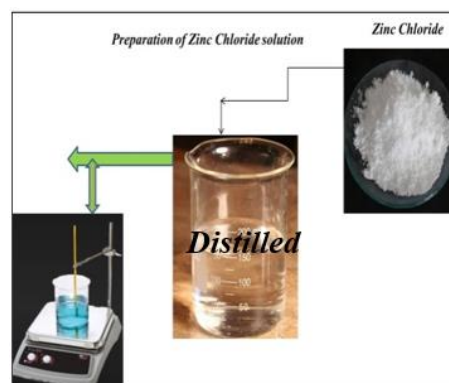


Fig. 2: Preparation of Zinc Chloride solution.

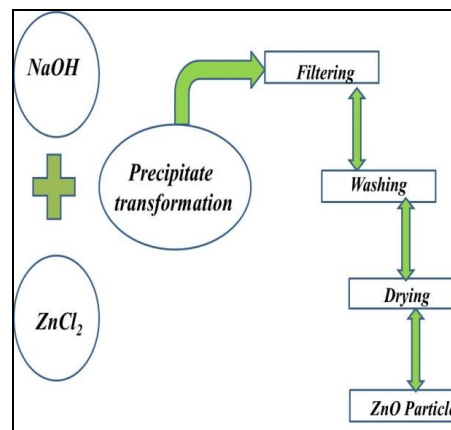


Fig. 3: Preparation of ZnO nanoparticle



Fig. 4: Prepared ZnO nanoparticle

**Synthesis of Copper oxide nano-particles by sol-gel technique:** Copper Chloride ( $\text{CuCl}_2$ ) and sodium hydroxide ( $\text{NaOH}$ ) were the two starting materials for preparation of Copper oxide nano particles. We took a 1.5 gm of  $\text{NaOH}$  in 40 ml ethanol and stirred it room temperature in a beaker on a magnetic stirrer. After that we took a 1 gm of copper chloride in ethanol in a beaker and stirred it on another magnetic stirrer.  $\text{NaOH}$  solution added in  $\text{CuCl}_2$  solution drop wise continuously and allowed to stirring for 30 minutes. The dropping of the  $\text{NaOH}$  solution in a copper chloride solution results in reaction occurs and color turns from dark blue to black. Filter paper is used to filter the gel and washed with water and sample allowed to dry at room temperature and it is color changes to dark brown.

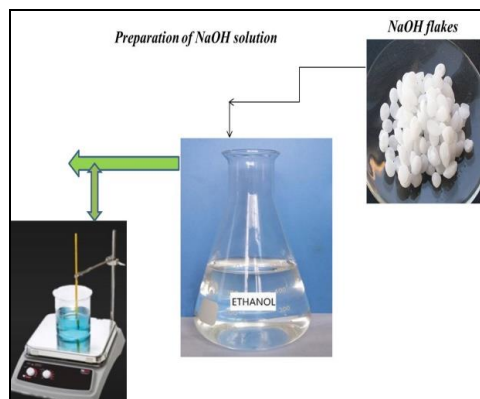


Fig. 5: Preparation of  $\text{NaOH}$  solution

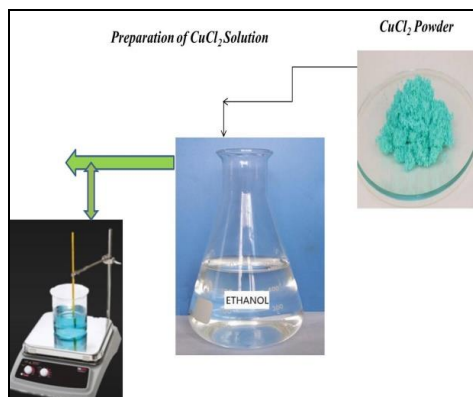


Fig. 6: Preparation of  $\text{CuCl}_2$  solution

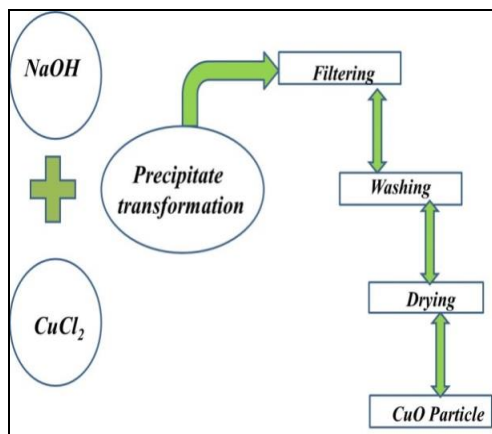


Fig. 7: Preparation of  $\text{CuO}$  particle



Fig. 8: Prepared  $\text{CuO}$  nano particle

**Synthesis of Zinc-Copper oxide particles by sol-gel technique:**  $\text{Zn-CuO}$  nano-structures were synthesized using the sol-gel method. The precursors, 2, 4, 6, 8, 10 gm of white anhydrous Zinc chloride and fixed 10 gm of blue copper chloride in weight percentage ratio were first powdered into a mortar with pestle for 20 minutes and then were kept in a different –different beaker. Then 20 ml of distilled water was gradually poured into this mixture contained in the beaker kept on a magnetic stirrer for a continuous stirring. After an hour when the mixture dissolved in the distilled water, we added ethanol (purity 99%) drop-wise into the beaker and the temperature was increased to  $60^\circ\text{C}$  to form sol. The reaction produced a solution of yellowish-green color with a tinge of blue. We kept it stirring for another four hours at room temperature while the whole mixture got dissolved in ethanol during this process. The precursors react with  $\text{OH}$  group of ethanol likewise. After this we left the solution to cool down, within several minutes, a reaction occurred showing a rapid formation of a rigid bluish green colored gel. Then the gel was dried at the same temperature. The obtained products were then rinsed multiple times by deionized water so that residual impurities are laid off. The gel now obtained was heated in an oven for about one hour at  $80^\circ\text{C}$  so that dried  $\text{Zn-CuO}$  powder is obtained.



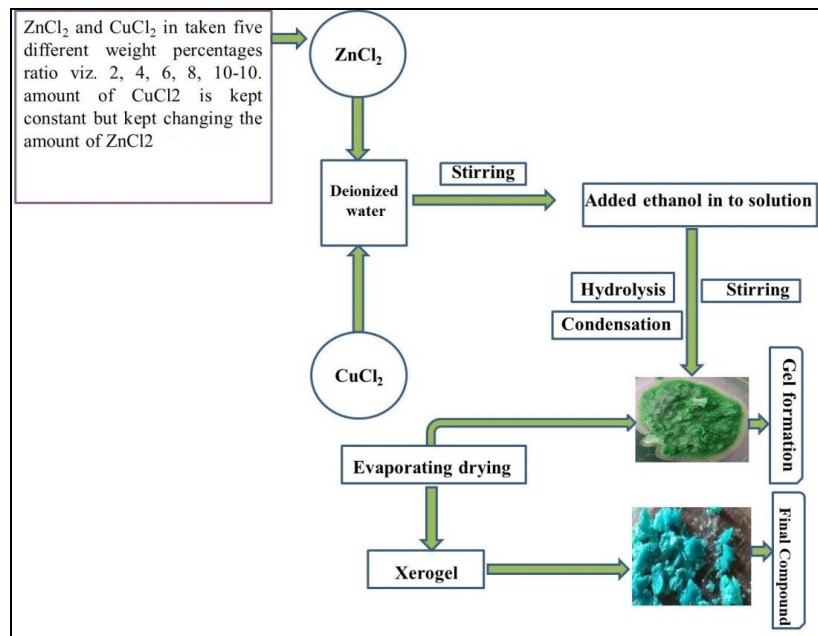


Fig. 9: Prepration of Zinc-Copper oxide particles

#### Synthesis of pure and Zn-CuO doped PMMA Films:

We took eight beakers of 100ml and in each a fixed amount of 1gm granule PMMA crystals were made to dissolve in 20ml dichloromethane and 5 ml of ethyl alcohol that acts as solvent. The molten PMMA is stirred uniformly in an ultra-sonicator for 6 hours at room temperature to assure the homogenous dispersion of polymer particles without concentricity throughout the solvent. After this, solution of one of the beaker was poured into a flat bottom petri dish of radius 3cm. The petri dish is placed floating on a layer of mercury so that the solution spreads homogeneously and film of uniform thickness can be obtained. Then we added

~.50 gm (weight percentage of 9%) of prepared ZnO, CuO, Zn-CuO particles into the solution of another beaker and allowed this to stir on a magnetic stirrer for 18 hours. When the nano-particles got completely dissolved in to the PMMA solution, we poured this solution into another glass flat bottom petri dish kept floated over mercury and left for 24 hours. Now the solvent is made to evaporate at room temperature and is left to dry as film in the petri dish which are then peeled off later. We obtained transparent PMMA film and white colored film of ZnO, Brown colored film of CuO, fluorescent yellow-green colored Zn-CuO doped PMMA film of 100µm thickness.

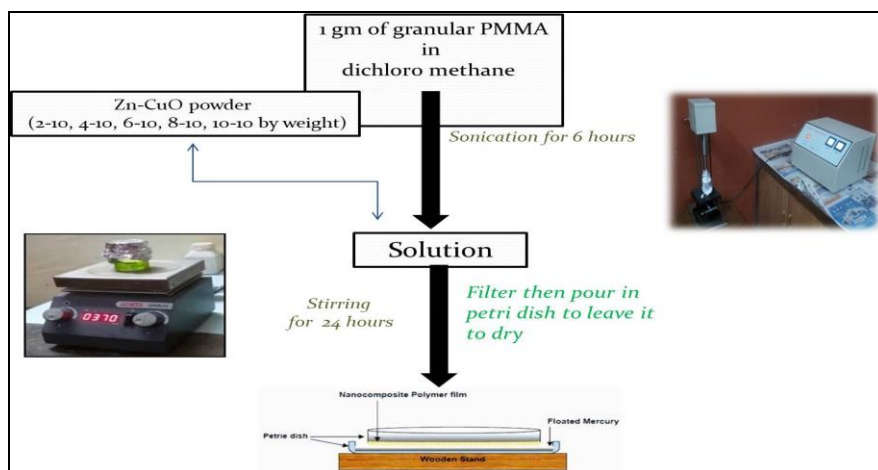


Fig. 10: Preparation of PMMA and Zn-CuO-PMMA composites.

**FTIR analysis:** The composition of functional groups of our synthesized powdered samples and prepared films were examined by FTIR Perkin Elmer Spectrum Version 10.4.00 FTIR Spectrophotometer within the region 400-4000 cm<sup>-1</sup> in material research facility (MNIT, Jaipur). Figure 11 shows the FTIR spectrum of the ZnO, CuO and Zn-CuO nanoparticles and doped in PMMA. The peak at 451 cm<sup>-1</sup> is that the characteristic absorption of Zn-O bond around 601, 508 and 487 cm<sup>-1</sup>, which may be assigned to the vibrations of Cu-O bonds. Other absorption peaks which corresponding the carboxylate and hydroxyl

impurities within the materials and same peaks are appearing within the each sample are shown in the graph. This result is good agreement with other works. (20) The broad absorption peak at around 3445cm<sup>-1</sup> is caused by the adsorbed water molecules since the nano crystalline materials exhibit a high surface to volume ratio and thus absorbs moisture and some hydrogen bonding interaction. (21) However with the incorporation of mixed metal oxides in PMMA, we see in figure 12 appearance of peak at 2949, 3445 cm<sup>-1</sup> indicating the functional group due to formation of the composite. Further, we observe that the intensity of

vibrational bands also increases. From these variations in intensity and appearance of characteristic peaks within the FTIR studies of our prepared films are ascertain that the chemical interaction between zinc-copper oxide has taken place coordinating with the carbonyl and methoxy oxygen of the polymer, we observe that the intensity of vibrational bands also increase.

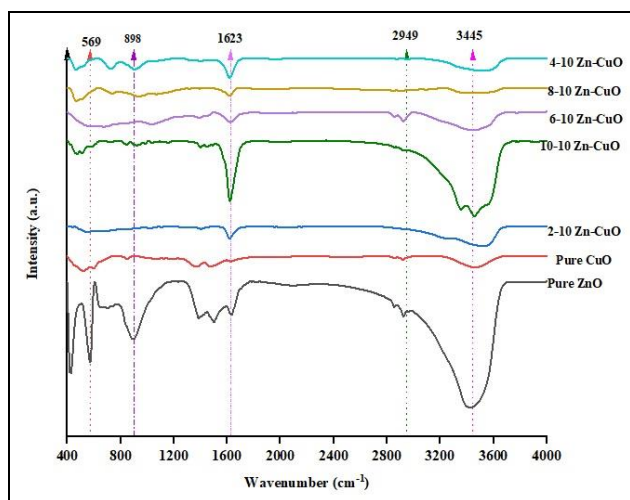


Fig. 11: FTIR spectrums of ZnO, CuO, Zn-CuO.

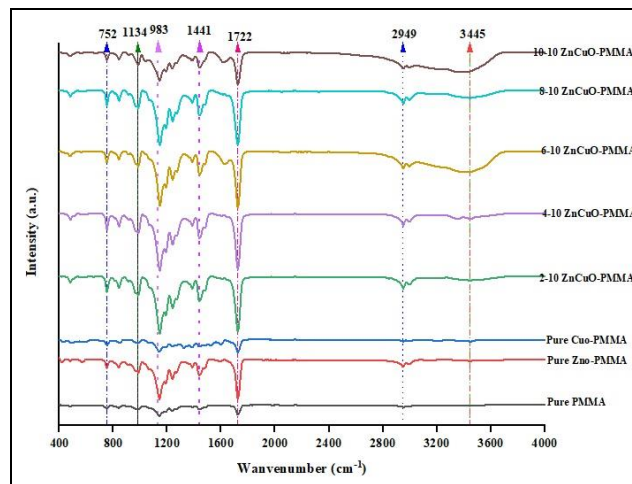


Fig. 11: FTIR spectrums of ZnO, CuO, Zn-CuO- PMMA composites.

**Scanning Electron Microscope:** The surface structure of the composite samples was investigated using S-3700N SEM scanning electron microscope in material research Centre (MNIT, Jaipur). The surface morphology of the prepared ZnO CuO and Zn-CuO nano particles was manifest through the SEM image shown in figure 13. It shows an identical distribution of particles of the prepared ZnO, CuO and Zn-CuO nanoparticles.

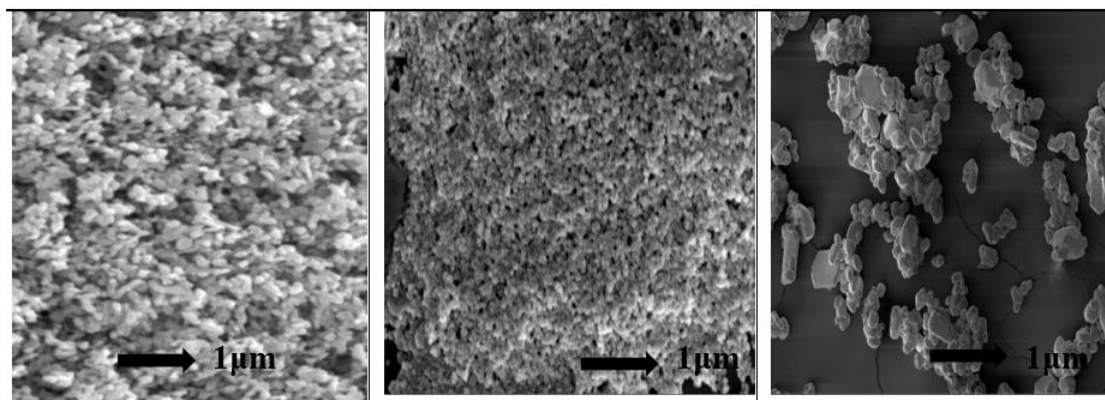


Fig. 13: SEM images of prepared CuO, ZnO and Zn-CuO nanoparticles.

**Characterization for investigation of optical parameters:** UV-Vis double beam spectrophotometer is an easiest device to test the optical properties to compute for band gap energy and to determine the sorts of electronic transition inside the materials. We have used EI 2375UV-Vis double beam spectrophotometer to record the absorbance spectra of the prepared sample films in the frequency range of 300–900 nm. Spectroscopy is the estimation and interpretation of electromagnetic radiation which is ingested or produced by a sample. This absorption happens when the molecules of the sample move starting with one energy state then onto the next within the incident light. It is a method which concentrates how light associates with matter/sample. Light is electromagnetic radiation which is comprised of discrete particles called photons. The spectrum used in spectroscopy varies from ultra-violet, visible, infrared ranges. The frequency range for the three spectra is 0-400, 400-700 or above. At the point when a light beams fall on sample, it gets retained partially, and remaining is reflected. The frequency of ingested light is explicit to the material taken. Spectroscopy

is stretched out to consider the substance dependent on their trademark absorbance of the spectra. At a given frequency, the force of light retained is relied upon the focus (amount) of the material. Where in the absorbance of a generalize frequency of light by the particles of the sample under test is resolved. The more the quantity of atoms in the sample, the higher is the absorbance and the other way around. Each sample has particles comprising of some functional groups by which they may cause tone or some nature to assimilate light of explicit frequency. This frequency at which test retains indeed is called as  $\lambda_{max}$ . At the point when the light beam is given to the sample, the electrons in the particles retain energy in the light and go for energized state. During this change, a portion of the light energy is ingested while the leftover light falls on the photo-electric detector.

**Theoretical consideration for evaluation of optical parameters:** The absorbance and transmittance spectra were recorded by double beam UV-Vis spectrophotometer within the wavelength of 300–800 nm at room temperature.

Once light of intensity ( $I$ ) is incident on a film of thickness ( $t$ ), relationship between incident intensity ( $I$ ) and penetrating light intensity ( $I_0$ ) is given by

$$I = I_0 \exp(-\alpha t) \quad (1)$$

So that

$$\alpha t = 2.303 \log I/I_0 \quad (2)$$

$$\text{Or coefficient of absorption } \alpha = 2.303(A/t) \quad (3)$$

Wherever  $\alpha$  is the absorption coefficient in  $\text{cm}^{-1}$  and therefore the  $I/I_0$  amount is defined as transmittance, so that  $\log(I_0/I)$  is the absorbance ( $A$ ).

The amount of optical energy gap from this region was evaluated from the Mott and Davis relation:

$$ah\nu = C(h\nu - E_g)^m \quad (4)$$

where  $h\nu = E$  is the energy of photon,  $C$  the proportional constant depending on the specimen structure,  $E_g$  is the allowed or forbidden energy gap of transition and the exponent  $m$  is an index, which determines the type of electronic transition responsible for absorption. It can take values  $1/2$ ,  $3/2$  for direct and  $2$ ,  $3$  for indirect allowed and forbidden transitions, respectively. Reported literature [7,8] suggests that if the amount of absorption  $\alpha > 10^4 \text{ cm}^{-1}$ , the electronic transitions is direct, otherwise indirect one. If plotting  $\alpha$  vs.  $E$  (i.e.,  $h\nu$ ) shows  $E^{1/2}$  dependence, then, plotting  $\alpha^2$  with  $E$  will show a linear dependence. Therefore, if a plot of  $h\nu$  vs.  $\alpha^2$  forms a line, it will unremarkably be inferred that there is a direct band gap, measurable by extrapolating the straight line to the  $\alpha = \text{zero}$  axis. On the opposite hand, if plotting  $\alpha$  vs.  $E$  (i.e.,  $h\nu$ ) shows  $\alpha E^2$  dependence, then, plotting  $\alpha^{1/2}$  with  $E$  will show

a linear dependence. So, when a plot of  $\alpha^{1/2}$  vs.  $h\nu$  forms a straight line, it can normally be inferred that there is a indirect band gap, measurable by extrapolating the straight line to the  $\alpha = 0$  axis. Further, the extinction coefficient is calculated using the relation:

$$k = \frac{\alpha \lambda}{4\pi} \quad (5)$$

Where  $\lambda$  is the wavelength of the incident ray. The reflectance  $R$  is obtained from absorbance  $A$  and Transmittance  $T$  using the following relation:

$$R + A + T = 1 \quad (6)$$

The refraction index ( $n$ ) was calculated using the relation:

$$n = \frac{(4R/(R-1)^2 - k^2)^{1/2} - (R+1/R-1)}{2} \quad (7)$$

Also, the finesse coefficient is given by:

$$F = \frac{4R}{(1-R)^2} \quad (8)$$

The real ( $\epsilon_r$ ) and imaginary ( $\epsilon_i$ ) parts of the dielectric constant are related to  $n$  and  $k$  values accordingly:

$$\epsilon_r = n^2 - k^2 \quad \text{and} \quad \epsilon_i = 2nk \quad (9)$$

The optical conductivity is related to light speed and can be expressed by the subsequent equation:

$$\sigma_{\text{opt}} = \frac{nc\alpha}{4\pi} \quad (10)$$

**Result and Discussion:** Figure 14 shows the absorbance spectra as a component of frequency of the incident light for PMMA film with various dopant materials. It is clear that for pure ZnO-PMMA composite, in the polymer matrix prompts increment in the peak intensity. Subsequently, there is chemical cooperation between the two segments in

the matrix and the addition in the retention is credited to the increment in the dopant material, which is the retaining (absorbing) component. Likewise increment in the intensity for dopant viz. pure CuO-PMMA, 2, 4, 6, 8, 10-10 Zn-CuO-PMMA composites shows more absorbance as compare to the pure PMMA composite. Pure PMMA film is profoundly transparent in nature in the uv-visible region however Pure ZnO, CuO and Zn-CuO/PMMA composites are shows less transparency in uv-visible area.

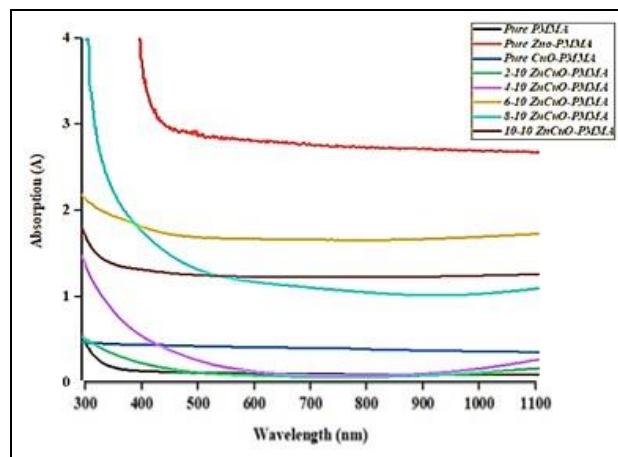


Fig. 14: Variation in absorption spectra with dopant material.

**Energy Band Gap Analysis:** Figure 15 shows coefficient of absorption ( $\alpha$ ) was calculated using equation 3. It can be seen that absorption  $\alpha$  relatively small on increasing wavelength because the possibility of electron transition is low, because the energy of the incident photon is not sufficient to move the electron from the valence band to the conduction band ( $h\nu < E_g$ ). At lower wavelength absorption is high meaning there is a bigger chance of electron transition [3]. Literature says, "When the values of the absorption coefficient are high ( $\alpha > 10^4$ )  $\text{cm}^{-1}$ , it is expected that direct transition of electron happens". On the opposite hand, when the values of the absorption coefficient are low ( $\alpha < 10^4$ )  $\text{cm}^{-1}$ , it is expected that indirect transition of electron occurs. [17-19] In figure 12 intercept if the linear curves to zero absorption on  $h\nu$  axis gives the value of optical energy band gap. It can be clearly seen that the value of optical energy band gap depend on the dopant material. There is a decrease in optical energy band gap value of composites compare to the pure PMMA composite that is shown in figure 15. The rate of the energy band gap with the different dopant of ZnO, CuO and Zn-CuO nanoparticles is inversed. Literature says, this can be due to the rise in the shift of the valence and the conduction band. The enhancement of carrier-carrier interaction due to the great concentration of carrier in valence and conduction bands prompts to a decrease in the band gap. other than that, the presence of unsaturated deformities caused an expansion in the density of localized states in the band gap and afterward decreased the optical energy gap compared to the pure PMMA composite. The decrement of the energy gap is equivalent to the pure PMMA composite. The decrement of the energy gap is equal to 1.17 eV with pure ZnO-PMMA composite and 0.10 eV with Pure CuO-PMMA. Because the figure 16 depicts that the variation shown within the energy gap is not uniform which is due to the energy being relative to the strains of Zn-CuO-PMMA.



Optical energy band gap values for all dopant material listed in the table-1.

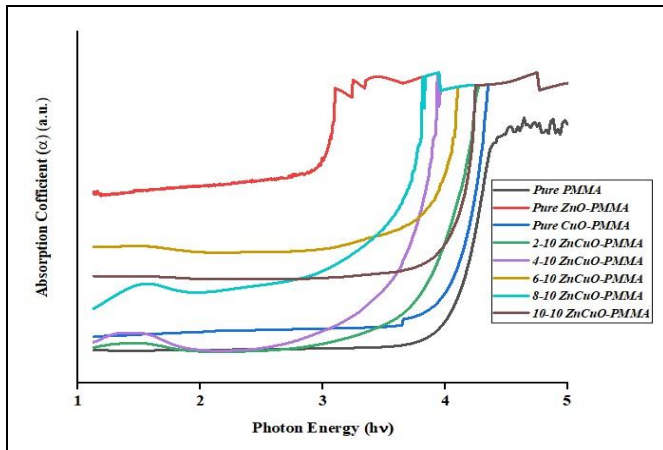


Fig. 15: variation of absorption coefficient ( $\alpha$ ) ( $\text{cm}^{-1}$ )

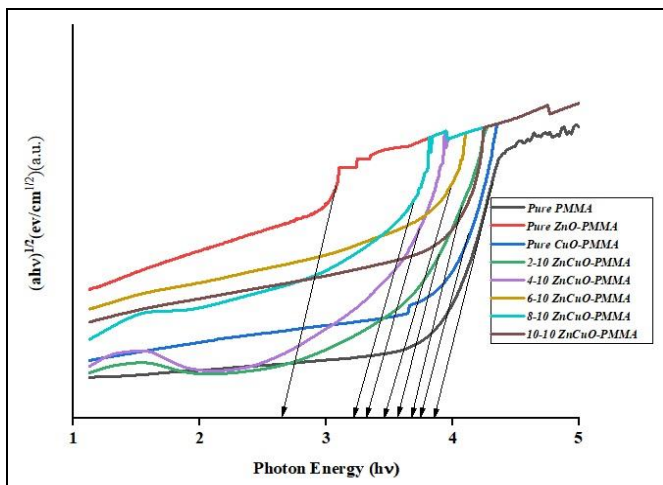


Fig. 16: Variation of optical energy band gap value

Dopant	Optical energy band gap (ev)
Pure PMMA	3.82
Pure CuO-PMMA	3.72
Pure ZnO-PMMA	2.65
2-10 ZnCuO-PMMA	3.60
4-10 ZnCuO-PMMA	3.33
6-10 ZnCuO-PMMA	3.42
8-10 ZnCuO-PMMA	3.24
10-10 ZnCuO-PMMA	3.68

**Refractive index, Extinction coefficient, Finesse coefficient, Dielectric constant:** The fundamental optical parameters like the extinction coefficient, refractive index, finesse coefficient and dielectric constant are necessary to be evaluated to understand the polarizability of the dopant materials, and their consequent applications.

**Extinction coefficient:**

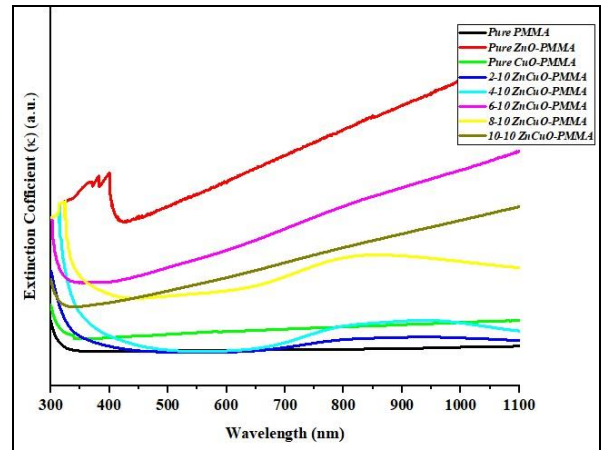


Fig. 17: variation in extinction coefficient ( $\kappa$ ).

The variation in  $\kappa$  is shown in figure 17 variation of the extinction coefficient of composites with photon energy for various dopant materials. It is seen that  $\kappa$  will increase with pure ZnO-PMMA, Pure CuO, 6, 8, 10-10 ZnCuO-PMMA and almost same behavior as pure PMMA for 2-10 ZnCuO-PMMA and 4-10 ZnCuO-PMMA composites, the extinction coefficient is increased with the rise of Zinc oxide particles in to dopant that attributed to the increase of absorb part of the incident light and so, loss of energy as a result of reaction between the light and the molecules of the medium. Same behavior was noted in ref. [13-14].

**Finesse coefficient (F):** Figure 18 shows the values of finesse coefficient against wavelengths at various dopants with reference to PMMA. The finesse coefficient decreases with increase in quantity of zinc in dopant materials. Owing to doped additives that lead to change in reflectance as  $F$  is dependent on  $R$ . It had been discovered that  $F$  values increase after a certain value at lower wavelengths [14] for Pure-PMMA, Pure CuO-PMMA, 2, 4-10 ZnCuO-PMMA composites sample. The positions of the peaks in the spectrum are also shifted as we tend to move towards the increase amount of ZnO doping in dopant material.

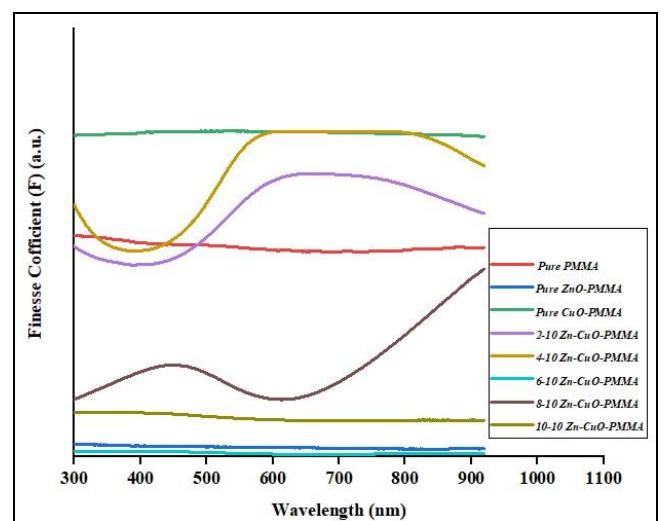


Fig. 18: Variation of Finesse coefficients ( $f$ )

**Refractive index ( $\eta$ ):** The relation between the refractive index of composites and wavelength is shown in figure 19. The values of refractive index can be obtained from the reflection coefficient  $R$  and extinction coefficient  $k$  data

using the Fresnel formulae defined through equation (6). The figure shows that the refractive index increases with the when amount of CuO is dominant in the dopant material, which is due to the increase in the scattering of light. [16] Figure 16 show that the refractive index decreases at the greatest wavelengths the observed increase in the refractive index due to incorporation of CuO in PMMA polymer. For ZnO-PMMA and 6, 8, 10-10 ZnCuO-PMMA composite which means higher amount of ZnO in dopant does not show the refractive index in uv-vis region wavelength.

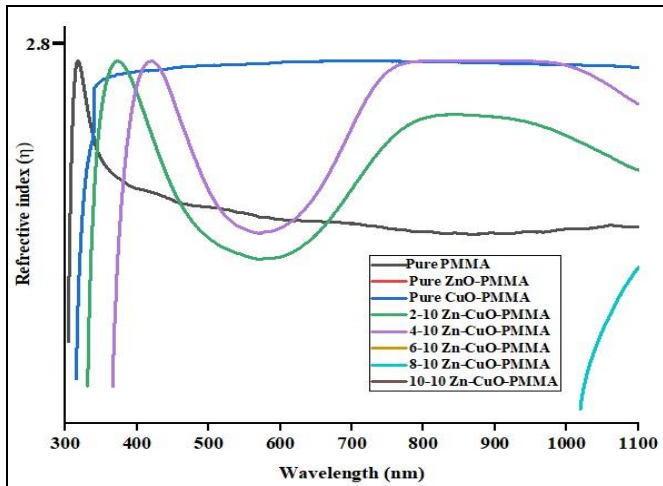
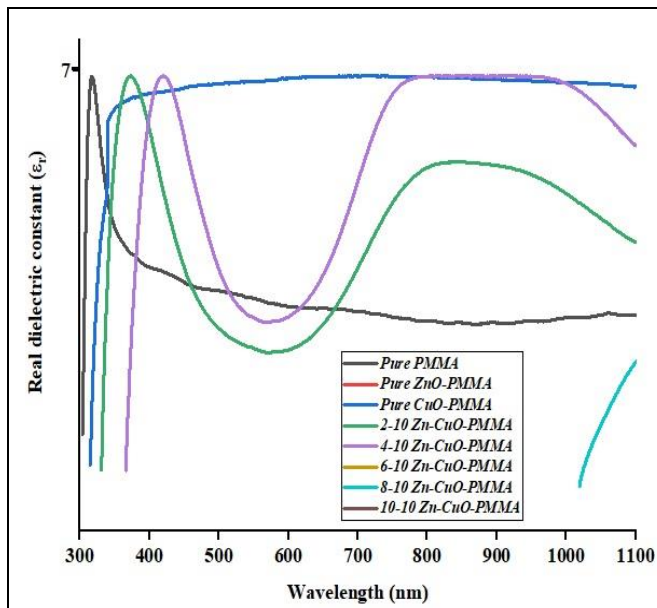
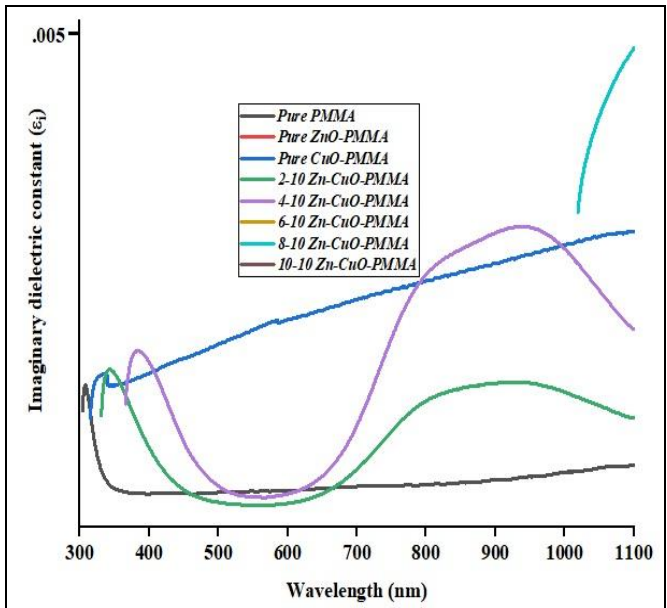


Fig. 19: Variation of refractive index ( $n$ ).



(a)



(b)

Fig. 20: (a) Variation of real part of dielectric constant (b) Variation of imaginary part of dielectric constant.

**Optical conductivity:** The optical conductivity ( $\sigma$ ) for pure PMMA- and dopant PMMA samples was estimated using the absorption coefficient  $\alpha$  and the refractive index  $n$  data using the relation expressed in equation (10). An increase in optical conductivity is ascertained on increasing the doping amount of CuO and some Zn-CuO in dopant material in PMMA and increase in photon energy as shown in figure 21. This aspect of optical conductivity was seen in ref. [15], where dopant substrate was PVA. But For ZnO-PMMA and 6, 8, 10-10 ZnCuO-PMMA composite that

**Dielectric Constant:** Figure (20 a) and figure (20 b) show the variation of real and imaginary parts of dielectric constant of dopant material composites with wavelength for different dopant of ZnO, CuO and ZnCuO in PMMA respectively. From the figures, the real and imaginary parts of dielectric constant for dopant composites increase with the increase of ZnO concentration. The increase of real and imaginary parts of dielectric constant attributed to increase the absorption of incident light and the density of dopant composites with the increase of Zinc oxide concentrations in dopant in PMMA similar to the behavior reported in references [13, 14]. But For ZnO-PMMA and 6, 8, 10-10 ZnCuO-PMMA composite that means higher amount of ZnO in dopant does not show the dielectric effect in uv-vis region wavelength.

means higher amount of ZnO in dopant does not show the optical behavior in uv-vis region wavelength.



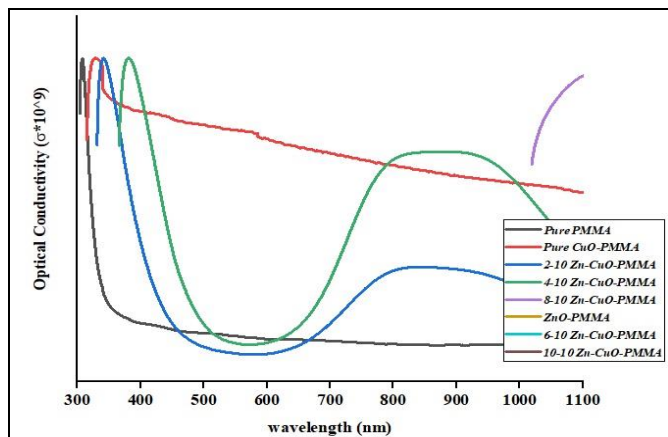


**Fig. 21:** Variation of optical conductivity

**Conclusion:** In this work, ZnO, CuO and Zn-CuO were prepared by sol-gel technique and solid polymer films of ZnO, CuO, and Zn-CuO-PMMA were prepared by the casting technique. Optical quantities such as absorption coefficient, optical energy gap, refractive index, optical conductivity, extinction coefficient and dielectric constants were determined from the absorbance of UV-visible spectra analysis. From the obtained results, it was found that the optical band gap energy extensively decreased with compare to the PMMA polymer thus, band gap can be plausibly tuned. The increase in optical conductivity of polymer upon the limited addition of ZnO, CuO is attributed to an increase in charge carrier concentration. The observed increase in refractive index and dielectric constant in the doped samples is related to added compound and are decisive for optoelectronics application. The results of the present work show that all the optical parameters are significantly affected by doping of ZnO, CuO and mix Zn-CuO.

#### References:

1. Kalotra P, Singh N, Dadhich A, Shrivastava S, Soni G and Vijay Y K 2019 *Adv. Sc. Eng. and Med.* 10 1.
2. Bafna M, Gupta A K, Khanna R K 2019 *Mater. Today:Proc.* MATPR7592
3. Bafna M, Gupta A K, Khanna R K, Vijay Y K 2018 *Bull. of Mat. Sc.* 41 160
4. Khodair Z T, Saeed M H and Abdul-Allah M H 2014 *Iraqi J of Phy* 12(24) 47
5. Najeeb H N, Dahash G A, Haddawi S F, and Jassim S M 2014 *Chem and Mater Eng* 2(6) 145
6. Bafna M and Garg N 2017 *J of Sc. and Tech.* 6(1) 27
7. Ramesan T M and Bijudas K 2016 *J. of Chem. & Pharm. Sc.* 1 52
8. Roaaramadan, Ramajaj E K, and Hasan A A 2014 *Int. J of Elec. Eng.* 2(3) 6
9. Choudhary S 2017 *Ind J of Chem tech*, 24 311
10. Bafna M, Gupta A K, Khanna R K 2018 *J. of Emer Tech. and Inno. Res.* 5(2) 433
11. Vijay S, Vijayavargiya J K, Sharma A and Vijay Y K 2013 *Amer. Sc Pub* 5 1
12. Bafna M, Garg N, Gupta A K 2018 *J. of Emer Tech. and Inno. Res.* 5(1) 494
13. Abdulallah M. H., Chiad S. S., Habubi N. F, Diyala *Journal for Pure Science*, 6 (2) (2010) 161-169.
14. Najeeb H. N., Balakit A.A., Wahab G. A. Kodeary A. K, *Acadmic Research Institute*, (2014) 48-56.

15. Abdullah O G, Shujahadeen B A and Rasheed M A 2016 *Results in physics* (Elsevier Publication) vol 6, p 1103.
16. Kittel C 2005 *Introduction to solid state physics* (USA: John Wiley & Sons) 8th edn
17. Ali B R and Kadhem F N 2013 *Int. J. Appl. Innov. Eng. Manag.* 2114
18. Abdullah O G, Shujahadeen B A and Rasheed M A 2016 *Results in physics* (ElsevierPublication) vol 6, p 1103
19. Khodair Z T, Saeed M H and Abdulallah M H 2014 *Iraqi J. Phys.* 1247
20. K. Hedayati, 2015, *journal of nanostructures*, 395-401
21. A. Radhakrishnan, B. Beena, *Indian Journal of Advances in Chemical Science* 2014, 158-161